Langmuir Article

pubs.acs.org/Langmuir

Interfacial Electronic Structure of Gold Nanoparticles on Si(100): Alloying versus Quantum Size Effects

Youngku Sohn,† Debabrata Pradhan, Abdullah Radi, and K. T. Leung*

WATLab, and Department of Chemistry, University of Waterloo, Waterloo, Ontario N2L 3G1, Canada. †Present address: Department of Chemistry, Yeungnam University, Gyeongsan, Gyeongbuk 712-749, South Korea

Received March 7, 2009. Revised Manuscript Received May 5, 2009

Gold nanoparticles (Au NPs) were prepared on a native-oxide-covered Si(100) substrate by sputter-deposition followed by thermal annealing. The size of Au NPs could be controlled in the range of 8−48 nm by varying the sputter-deposition time and post-annealing temperature. The interparticle separation was found to be directly related to the size of Au NPs, with smaller separations for particles of smaller size. The surface morphology, crystal structure, and interfacial composition of the chemical states of these supported Au NPs were studied as a function of their average size by using scanning electron microscopy, glancing-incidence X-ray diffraction, and depth-profiling X-ray photoelectron spectroscopy (XPS), respectively. The new Au $4f_{7/2}$ peak found at 1.1−1.2 eV higher in binding energy than that for the metallic Au feature (at 84.0 eV) can be attributed to the formation of Au silicide at the interface between Au NPs and the Si substrate. Depth-profiling XPS experiments revealed no discernible change in the binding energies of the Au silicide and metallic Au 4f features with increasing Ar^+ sputtering time, indicating that the Au-to-silicide interface is abrupt. Furthermore, the shift in the Au $5d_{5/2}$ valence band to a higher binding energy and the reduction of the Au 5d spin−orbit splitting with increasing Ar^+ sputtering time also support the formation of Au silicide. No clear evidence for the quantum size effect was observed for the supported NPs. The finite density of state at the Fermi level and the fixed Au $4f_{7/2}$ peak position clearly indicate the metallic nature of the Au silicide at the Au−Si interface.

1. Introduction

Gold is a very important metal not only as an excellent electrical conductor but also as a nonreactive metal in its bulk state. In modern electronic devices, Au has been extensively used as an indispensable electrode material.[1,2] The physical properties of Au greatly depend on the sizes (or coordination numbers) and structures.[3−8] The electronic properties of Au in the nanometer-size regime are dramatically different from those of the bulk. Au also becomes chemically reactive as the size decreases, and Au nanoparticles (NPs) have therefore emerged as a new active catalyst.[9−13] In recent years, substantial efforts have been devoted to study the catalytic activity of Au NPs supported on oxide substrates and to understand the effects of NP size and substrate.[5−22] For example, Chen and Goodman studied the activity of Au NPs supported on titanium oxides toward CO oxidation, and attributed the high catalytic activity of Au NPs to both structural (e.g., particle size) and substrate effects.[15]

Both X-ray and ultraviolet photoelectron spectroscopy (XPS and UPS) have been employed to study the quantum size and substrate effects of Au NPs supported on various substrates.[16−25] The real question here is whether the binding energies (BEs) of the core-level states (e.g., Au 4f) and the density of states (DOS) of the valence band (VB) near the Fermi level (e.g., Au 5d) of the Au NPs are affected by the quantum size effect or the substrate effect, or both. For Au NPs supported on a substrate, three possible scenarios can be envisioned: (1) *Substrate effect*: As the particle size decreases, the proportion of the total number of atoms in each NP in direct contact with the surface of the substrate increases. In such case, the electronic structure of NPs could be significantly influenced by the substrate. (2) *Quantum size effect*: In the case where the NPs are electronically well isolated from the substrate, the electrons are confined inside the NPs. The electronic properties should therefore be affected only by the decreasing size of the NPs. (3) *Alloying effect*: NPs could form an alloy with the substrate, therefore changing the crystal structure of the original Au lattice and the corresponding electronic structure. For all three cases, the electrons in the VB are redistributed.

*Corresponding author. E-mail: tong@uwaterloo.ca.

(1) Goodman, P. *Gold Bull.* **2002**, *35*, 21.
(2) Yu, H.-Z. *Chem. Commun.* **2004**, *23*, 2633.
(3) Della Pina, C.; Falletta, E.; Prati, L.; Rossi, M. *Chem. Soc. Rev.* **2008**, *37*, 277.
(4) Bond, G. C.; Louis, C.; Thompson, D. T. *Catalysis by Gold*; Imperial College Press: London, 2006; Vol. *6*.
(5) Haruta, M. *Catal. Today* **1997**, *36*, 153.
(6) Rao, C. N. R.; Kulkarni, G. U.; Thomas, P. J.; Edwards, P. P. *Chem.—Eur. J.* **2002**, *8*, 29.
(7) Daniel, M.-C.; Astruc, D. *Chem. Rev.* **2004**, *104*, 293.
(8) Lemire, C.; Meyer, R.; Shaikhutdinov, S.; Freund, H.-J. *Angew. Chem., Int. Ed.* **2004**, *43*, 118.
(9) Hashmi, A. S. K.; Hutchings, G. J. *Angew. Chem., Int. Ed.* **2006**, *45*, 7896.
(10) Meyer, R.; Lemire, C.; Shaihutdinov, Sh. K.; Freund, R. *Gold Bull.* **2004**, *37*, 72.
(11) Hutchings, G. J. *Catal. Today* **2005**, *100*, 55.
(12) Bond, G. C. *Catal. Today* **2002**, *72*, 5.
(13) Corti, C. W.; Holliday, R. J.; Thompson, D. T. *Appl. Catal., A* **2005**, *291*, 253.
(14) Bell, A. T. *Science* **2003**, *299*, 1688.
(15) Chen, M. S.; Goodman, D. W. *Science* **2004**, *306*, 252.
(16) Guczi, L.; Peto, G.; Beck, A.; Frey, K.; Geszti, O.; Molnar, G.; Daroczi, C. *J. Am. Chem. Soc.* **2003**, *125*, 4332.
(17) Haruta, M.; Date, M. *Appl. Catal., A* **2001**, *222*, 427.
(18) Ono, L. K.; Roldan Cuenya, B. *J. Phys. Chem. C* **2008**, *112*, 4676.
(19) Liu, H.; Mun, B. S.; Thornton, G.; Isaacs, S. R.; Shon, Y.-S.; Ogletree, D. F.; Salmeron, M. *Phys. Rev. B* **2005**, *72*, 155430.
(20) Balamurugan, B.; Maruyama, T. *Appl. Phys. Lett.* **2005**, *97*, 143105.
(21) Takahiro, K.; Oizumi, S.; Terai, A.; Kawatsura, K.; Tsuchiya, B.; Nagata, S.; Yamamoto, S.; Naramoto, H.; Narumi, K.; Sasase, M. *J. Appl. Phys.* **2006**, *100*, 084325.
(22) Lopez-Salido, I.; Lim, D. C.; Dietsche, R.; Bertram, N.; Kim, Y. D. *J. Phys. Chem. B* **2006**, *110*, 1128.
(23) Zhang, P.; Sham, T. K. *Phys. Rev. Lett.* **2003**, *90*, 245502.
(24) Dalacu, D.; Klemberg-Sapieha, J. E.; Martinu, L. *Surf. Sci.* **2001**, *472*, 33.
(25) Wertheim, G. K.; DiCenzo, S. B.; Youngquist, S. E. *Phys. Rev. Lett.* **1983**, *51*, 2310.

Consequently, the spin−orbit splitting and width of the Au 5d bands would generally become smaller if at least one of the aforementioned scenarios is effective. In practice, it is very difficult to differentiate these three effects from the VB spectrum alone. The positions of Au 4f core-level BEs can be used to reflect the initial and final state effects in the photoemission process. For the final-state effect, the Au 4f level generally shifts to a higher BE position with a broadened width as the NP size decreases.[25] In the case of the substrate or alloying effect, the Au 4f level shifts to a higher or lower BE depending on the charge transfer direction (chemical shift). It may therefore be possible, in appropriate cases, to distinguish these three effects upon careful analysis of the core-level XPS spectrum.

Understanding the interfacial electronic structure and bonding of Au NPs on Si may provide insights into development of new applications in nanocatalysts and Si-based nanoelectronics. Au NPs can be produced on a Si substrate by various techniques, including electro and electroless solution based chemistry[26−29] and vapor deposition methods.[30−32] In the present work, size-specific Au NPs were prepared on a Si(100) substrate by a simple technique involving sputter-deposition followed by thermal annealing.[33,34] The surface morphology, crystal structure, and interfacial composition of chemical states were studied as a function of the Au NP size by using scanning electron microscopy (SEM), glancing-incidence X-ray diffraction (GIXRD), and depth-profiling XPS, respectively.

2. Experimental Details

Au films of different thicknesses were deposited on native-oxide-covered Si(100) substrates by varying the sputter-deposition time using a magnetron sputter-coater (Denton Desk II). The Si substrates (15×2.5 mm^2) were cut from a single-side-polished, p-type boron-doped Si(100) wafer (0.4 mm thick, purchased from Waferworld) with a resistivity of 1.0−1.5 mΩ cm. The as-deposited Au films were then annealed in air at various temperatures in a conventional oven for 1 h to produce the Au NPs of specific size distributions. The surface morphology of the NPs was characterized by using a LEO 1530 field-emission scanning electron microscope. The crystal structures of the Au NPs supported on a Si substrate were checked by GIXRD using a high-resolution four-circle X-ray diffractometer (PANalytical X'Pert Pro MRD), with the Cu Kα (1.542 Å) anode operating at 45 kV and 40 mA and positioned at an incident angle of 0.6° from the sample surface. Their corresponding chemical states over depth were analyzed by using XPS as a function of Ar^+ ion sputtering time. In particular, XPS measurement was first performed on the as-prepared sample, followed by sequential cycles of Ar^+ ion sputtering for a predetermined period followed by XPS measurement. For these depth-profiling XPS studies, we used a Thermo-VG Scientific ESCALab 250 microprobe with a monochromatic Al Kα source (1486.6 eV) with a typical energy resolution of 0.4−0.5 eV full width at half-maximum (fwhm). For the Ar^+ sputtering, an ion beam with an incident energy of 3 keV was directed over a 3×3 mm^2 rastered sample area, producing an approximate sputtering rate of 0.6 nm/min for Au with an ion current density of 0.3−0.4 μA/mm^2. Details of the analysis procedures have been given in our earlier work.[26]

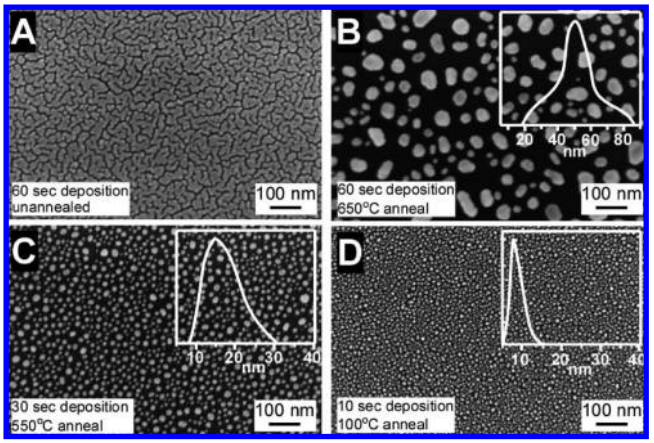

Figure 1. SEM images for (A) a 10 nm thick Au film obtained by sputter-deposition for 60 s, and Au nanoparticle samples obtained with different respective combinations of sputter-deposition time and post-annealing temperatures (for 1 h) of (B) 60 s and 650 °C, (C) 30 s and 550 °C, and (D) 10 s and 100 °C. Corresponding particle size distributions for the NP samples are shown as insets.

3. Results and Discussion

By controlling the Au film thickness with a different amount of sputter-deposition time and judicious choice of the post-annealing temperature, Au NPs of different size distributions could be easily obtained. In general, the average size of the Au NPs increases with increasing Au film thickness and increasing post-annealing temperature (and/or time). Figure 1 shows the SEM images for a 10 nm thick Au film prepared by sputter-deposition for 60 s (sample A) and Au NP samples of three different size distributions (shown as insets): 30−70 nm (sample B), 10−30 nm (sample C), and 6−12 nm (sample D), obtained by appropriate combinations of the sputter-deposition time and post-annealing temperature. All the samples (both the film and NPs) were supported on Si(100) substrates covered by native oxide. Evidently, a larger sputter-deposition time increased the thickness of the deposited Au film, which led to a larger particle size upon post-annealing (Figure 1B−D). To achieve a smaller average size distribution such as that of sample D, a thinner film was annealed with the lowest possible post-annealing temperature to induce nucleation. In addition, the separations between Au NPs were also found to be directly related to the size of Au NPs. A higher post-annealing temperature induced stronger agglomeration of Au atoms, forming bigger droplets, resulting in larger separations in between the NPs (Figure 1B). Similarly, a lower post-annealing temperature produced weaker agglomeration, thereby forming smaller Au NPs and smaller interparticle separations (Figure 1D). It is important to note that the average size distribution and interparticle separations of the Au NPs are very important for controlling the diameters and spacing in catalytic growth of nanowires.[35]

Figure 2 compares the corresponding GIXRD patterns for the 10 nm thick Au film and the three Au NP samples. These patterns are found to be in good accord with the face-centered cubic (fcc) metallic Au reference (JCPDS 65-2870), with the relative intensities of individual XRD features of all the samples found to be

(26) Zhao, L.; Siu, A. C.-L.; Petrus, J. A.; He, Z.; Leung, K. T. *J. Am. Chem. Soc.* **2007**, *129*, 5730.
(27) Oskam, G.; Searson, P. C. *J. Electrochem. Soc.* **2000**, *147*, 2199.
(28) Magagnim, L.; Maboudian, R.; Carraro, C. *J. Phys. Chem. B* **2002**, *106*, 401.
(29) Ali, H. O.; Christie, I. R. A. *Gold Bull.* **1984**, *17*, 118.
(30) Compagnini, G.; D'Urso, L.; Cataliotti, R. S.; Puglisi, O.; Scandurra, A.; La Fata, P. *J. Phys. Chem. C* **2007**, *111*, 7251.
(31) Landree, E.; Grozea, D.; Collazo-Davila, C.; Marks, L. D. *Phys. Rev. B* **1997**, *12*, 7910.
(32) Sekar, K.; Kuri, G.; Satyam, P. V.; Sundaravel, B.; Mahapatra, D. P.; Dev, B. N. *Phys. Rev. B* **1995**, *20*, 14330.
(33) Chang, J. F.; Young, T. F.; Yang, Y. L.; Ueng, H. Y.; Chang, T. C. *Mater. Chem. Phys.* **2004**, *83*, 199.
(34) Ruffino, F.; Bongiorno, C.; Giannazzo, F.; Roccaforte, F.; Raineri, V.; Grimaldi, M. G. *Nanoscale Res. Lett.* **2007**, *2*, 240.
(35) Ito, D.; Jespersen, M. L.; Hutchison, J. E. *ACS Nano* **2008**, *2*, 2001.

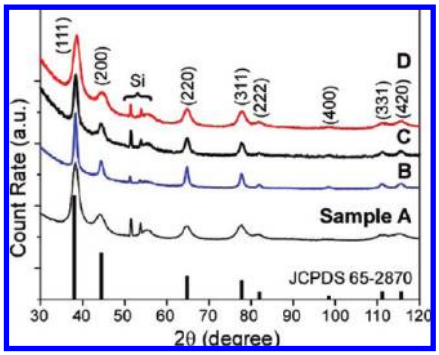

Figure 2. GIXRD patterns for (A) a 10 nm thick Au film obtained by sputter-deposition for 60 s, and Au nanoparticle samples obtained with different respective combinations of sputter-deposition time and post-annealing temperatures (for 1 h) of (B) 60 s and 650 °C, (C) 30 s and 550 °C, and (D) 10 s and 100 °C. The features at 50−60° correspond to the (311) plane of Si (JCPDS 27-1402). These patterns are compared with those of Au reference (JCPDS 65-2870).

not only nearly identical to one another but also closely resembling that of the reference spectrum. These patterns therefore confirm the random orientation of the polycrystalline NP growth. Spadavecchia et al. observed a very similar XRD pattern to ours for a Au film deposited on Si(100) annealed at 814 °C.[36] The Au NPs prepared in a $AuCl_3$ solution by electrodeposition and electroless deposition by us in an earlier study also exhibited nearly identical XRD patterns.[26] Evidently, the larger NPs (Figure 1B) exhibit a discernibly narrower XRD features than the smaller NPs (Figure 1C, D). The average grain sizes of the Au nanocrystallites estimated from the (111) diffraction feature by Scherrer analysis also follow an ascending trend with increasing NP size, from 6 to 7 nm (sample D) to 12−13 nm (sample C) and to 25 nm (sample B) [with the 6 nm crystals found for the Au film (sample A)]. These observations are consistent with the increasing post-annealing temperature employed for the preparation of these NP samples.

Detailed depth-profiling XPS analyses were carried out on the 10 nm thick Au film and the Au NP samples with different average size distributions. Figure 3 compares the XPS spectra of the Au 4f region for the four samples as a function of Ar^+ sputtering time. Based on the XPS data, we present schematic models, in Figure 4, for the formation and size evolution of Au NPs resulting from Ar^+ sputtering on the Si substrate. For the as-prepared samples, a weak C 1s feature at 285.0 eV was observed in all the XPS spectra (not shown), which indicates the presence of a minor carbonaceous component commonly found as a result of sample handling in air. The C 1s feature could be completely removed after sputtering for 5 s, which also resulted in an intensity increase in other XPS features. For the "clean" Au film obtained after 5 s sputtering (Figure 3A), the Au $4f_{7/2}$ ($4f_{5/2}$) peak at 84.0 eV (88.8 eV), with a fwhm of 0.8 eV, is assigned to metallic gold.[37] The intensities of metallic Au 4f peaks become weaker without any change in the BE position with increasing sputtering time to 60 s and appear to be totally removed after 120 s of sputtering. A new broader Au $4f_{7/2}$ ($4f_{5/2}$) peak at 85.1 eV (88.8 eV), 1.1 eV higher in BE than that of the metallic Au, is found to emerge after sputtering for 30 s and becomes stronger after sputtering for 120 s. Upon further sputtering, the new Au 4f peak is found to be slightly shifted by +0.2 eV to the higher BE side, along with reduction in intensity. Although this BE shift could be due to either a change in interfacial composition or a quantum size effect, this shift is not significantly larger than the experimental uncertainty (±0.1 eV). For the larger Au NPs in samples B and C (Figure 1), the corresponding Au 4f spectral evolutions with sputtering time are found to be very similar to that of the Au film (sample A). Furthermore, the onsets of the new Au 4f peak for the larger NPs appear at a later sputtering time, from 5 s (sample D) to 15 s (sample C) and 30 s (sample B), which is consistent with a proportionally thicker Au component on top of the Au silicide.

To identify the nature of the new Au 4f feature located at the higher BE, we first consider the quantum-size effect. It is important to note that the use of Ar^+ sputtering would gradually reduce the size of the as-prepared NPs with increasing sputtering time in our depth-profiling XPS experiments (Figure 4c). Extremely small NPs in the quantum size regime could therefore be produced on the Si substrate with this procedure. As the Au cluster size decreases, Au is expected to become nonmetallic.[25] The nonconducting nature of the Au NPs on the substrate should lead to positively charged Au NPs in the final state during the photoemission process, causing a shift toward higher BE and broadening of the 4f spectral feature.[25] This is consistent with the work by DiCenso et al., who reported no extra Au 4f feature and found that the Au 4f peak gradually shifts to a higher BE as the Au cluster deposited on an amorphous C substrate becomes smaller.[38] Bittencourt et al. also observed a gradual Au 4f BE shift, along with peak broadening, with decreasing size for Au clusters deposited on multiwall carbon nanotubes.[39] They attributed the BE shift to a quantum size effect.[38,39] Zhang and Sham prepared thiol-capped Au NPs on a conductive carbon substrate,[23] and observed that the Au 4f peak shifts by 0.36 eV, with asymmetric broadening of the peak at the higher BE side. They claimed that the observed shift was due to an initial-state substrate electronic effect, although such a shift could also be argued as the result of a final-state Coulomb charging effect.[40,41]

For Au deposited on an oxide-covered Si substrate, Dalacu et al. observed, unlike other XPS results that showed an additional Au $4f_{7/2}$ feature,[26,42−47] a gradual shift of the Au 4f peak from 84.0 to 85.0 eV with decreasing Au cluster size, accompanied by peak broadening, which they attributed to a cluster charging effect.[24] Peto et al. prepared a Au film on an oxide-covered Si(100) substrate by thermal evaporation and followed the spectral changes after two sputtering steps.[48] They also observed a shift of the Au 4f peak to a higher BE with increasing sputtering time, which they attributed to the size effect. However, because they performed only two sputtering steps, it is unclear whether the Au 4f BE shift is gradual. In the present work, our Au 4f spectra for the Au NPs (Figure 3) clearly show the evolution of an extra

(36) Spadavecchia, J.; Prete, P.; Lovergine, N.; Tapfer, L.; Rella, R. *J. Phys. Chem. B* **2005**, *109*, 17347.
(37) *Handbook of X-ray Photoelectron Spectroscopy*; Chastain, J., Ed.; Perkin-Elmer Corporation: Eden Prairie, MN, 1992
(38) DiCenzo, S. B.; Berry, S. D.; Hartford, E. H. *Phys. Rev. B* **1988**, *38*, 8465.
(39) Bittencourt, C.; Felten, A.; Douhard, B.; Ghijsen, J.; Johnson, R. L.; Drube, W.; Pireaux, J.-J. *Chem. Phys.* **2006**, *328*, 385.
(40) Moriaty, P. *Phys. Rev. Lett.* **2004**, *92*, 109601.
(41) Zhang, P.; Sham, T. K. *Phys. Rev. Lett.* **2004**, *92*, 109602.
(42) Sundaravel, B.; Sekar, K.; Kuri, G.; Satyam, P. V.; Dev, B. N.; Bera, S.; Narasimhan, S. V.; Chakraborty, P.; Caccavale, F. *Appl. Surf. Sci.* **1999**, *137*, 103.
(43) Sarkar, D. K.; Bera, S.; Dhara, S.; Narasimhan, S. V.; Chowdhury, S.; Nair, K. G. M. *Solid State Commun.* **1998**, *105*, 351.
(44) Khalfaoui, R.; Benazzouz, C.; Guittoum, A.; Tabet, N.; Tobbeche, S. *Vacuum* **2005**, *78*, 223.
(45) Lu, Z. H.; Sham, T. K.; Norton, P. R. *Solid State Commun.* **1993**, *85*, 957.
(46) Yeh, J. J.; Hwang, J.; Bertness, K.; Friedman, D. J.; Cao, R.; Lindau, I. *Phys. Rev. Lett.* **1993**, *70*, 3768.
(47) Molodtsov, S. L.; Laubschat, C.; Kaindl, G.; Shikin, A. M.; Adamchuk, V. K. *Phys. Rev. B* **1991**, *44*, 8850.
(48) Peto, G.; Molnar, G. L.; Paszti, Z.; Geszti, O.; Beck, A.; Guczi, L. *Mater. Sci. Eng., C* **2002**, *C19*, 95.

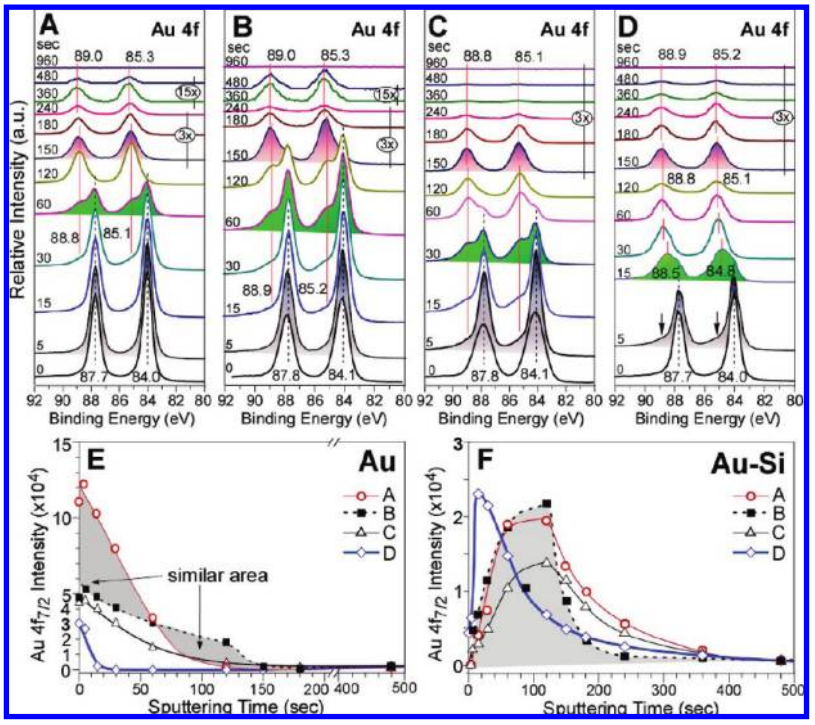

Figure 3. Au 4f spectra obtained as a function of Ar^+ sputtering time for (A) a 10 nm thick Au film obtained by sputter-deposition for 60 s, and Au nanoparticle samples obtained with different respective combinations of sputter-deposition time and post-annealing temperatures (for 1 h) of (B) 60 s and 650 °C, (C) 30 s and 550 °C, and (D) 10 s and 100 °C, and the corresponding depth profiles of Au $4f_{7/2}$ intensity for (E) the metallic Au feature at 84.0−84.1 eV and (F) Au silicide feature at 85.1−85.3 eV.

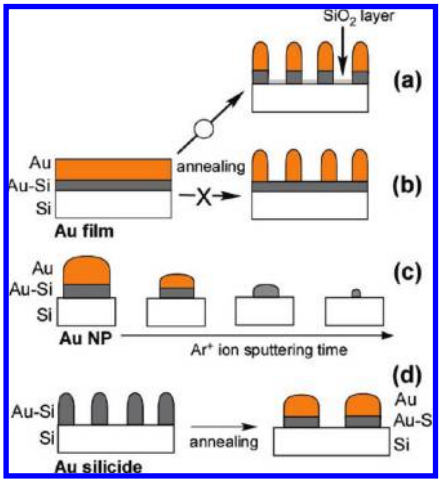

Figure 4. Schematic models of (a) probable and (b) improbable formation of Au NP on a Si substrate by thermal annealing of Au film; (c) size reduction of Au NPs as the result of increasing Ar^+ sputtering time; and (d) phase-separation of Au silicide particles to metallic Au and Au silicide upon thermal annealing.

Au 4f feature at the higher BE position, with its peak position and fwhm remaining unchanged with sputtering time, and without the metallic Au 4f feature shifting to a higher BE. We therefore conclude that the new Au 4f feature at 85.1−85.3 eV is not due to a quantum size effect but to the formation of a Au−Si alloy, that is, Au silicide. In addition, given the well-defined BE positions of the metallic peak and the new peak and the rather short amount of sputtering time needed for the transition from the metallic to the new feature, the interface between Au and Au silicide appears to be abrupt.[32,42]

The assignment of the new Au 4f XPS peak located at 1.1−1.2 eV higher in BE than that of metallic Au to Au silicide is consistent with the earlier studies.[26,42−47] In particular, for Au films (supported on Si substrates) irradiated by a high energy ion beam (120−350 keV, compared with the much lower 3 keV energy used in the present work), Sarkar et al.[43] and Khalfaoui et al.[44] observed a new broader Au 4f peak at 0.6 and 1 eV higher BE than that of metallic Au, respectively. Sundaravel et al. also observed a new broader peak at 1.2 eV higher BE than that of metallic Au for a sputtered Au film on Si(111).[42] These researchers all attributed the new feature to Au silicide. Similarly, by gradually increasing the Au coverage on a Si substrate at room temperature, other researchers observed a new Au 4f peak at a higher BE for a very low coverage and assigned the observed peak also to Au−Si alloy.[45−47,49] Furthermore, studies employing other experimental techniques,[33,42,44,50−52] such as Auger electron spectroscopy, also show characteristics of Au silicide at the Au−Si interface. For Au NPs (with an average diameter of 10.5 nm) obtained on a H-terminated Si(100) substrate by electrodeposition and electroless deposition in a $AuCl_3$ + $NaClO_4$ solution, we also observed a new, well-defined Au silicide $4f_{7/2}$ peak at 1.0 eV higher BE than the metallic Au.[26] In this earlier work, we could rule out the sputtering effect by removing the top Au component by dipping the sample in a diluted HF solution to expose the Au silicide interface (without sputtering). The remaining Au 4f peak observed at the higher BE indicates that the Au silicide form is indeed an interfacial property.[26] We can also rule out the assignment of Au^{3+} (as in Au_2O_3) for the new Au $4f_{7/2}$ peak because the calculated surface atomic ratio Au/O was found to be considerably larger than the expected value for Au_2O_3.

(49) Braicovich, L.; Garner, C. M.; Skeath, P. R.; Su, C. Y.; Chye, P. W.; Lindau, I.; Spicer, W. E. *Phys. Rev. B* **1979**, *20*, 5131.
(50) Green, A. K.; Bauer, E. *J. Appl. Phys.* **1976**, *47*, 1284.
(51) Dallaporta, H.; Cros, A. *Surf. Sci.* **1986**, *178*, 64.
(52) Ceelen, W. C. A. N.; Moest, B.; de Ridder, M.; van Ijzendoorn, L. J.; Denier van der Gon, A. W.; Brongersma, H. H. *Appl. Surf. Sci.* **1998**, *134*, 87.

It is of interest to examine the spectral evolution of NPs with the smallest size distribution (sample D) obtained in the present work in the initial stage of Ar^+ sputtering. Upon sputtering for just 5 s (Figure 3D), the Au $4f_{7/2}$ peak becomes asymmetric due to the emergence of a new shoulder feature at the higher BE side. After further sputtering to 15 s, the peak becomes significantly broader (with a fwhm of 1.7 eV) and shifts to a higher BE of 84.8 eV. If we were to base our conclusion solely on the development of asymmetry, broadening, and gradual shift to a higher BE in an XPS spectral feature without a careful analysis, we would have mistaken the observed spectral changes as manifestation of a quantum size effect.[16,48] A detailed depth-profiling study is therefore vitally important to fully characterize the nature of emerging new core-level features.

For small Au clusters with one to seven atoms deposited on a native-oxide-covered Si substrate, Cox et al. observed a Au $4f_{7/2}$ peak at ~1.0 eV higher BE than the corresponding metallic Au peak and attributed this BE shift to the nonmetallic nature of small Au clusters.[53] This conclusion is in marked contrast to that reported by Compagnini et al., who prepared mixed Au−Si nanoclusters of 2 nm and observed a broad Au $4f_{7/2}$ feature (with 1.7 eV fwhm) and a BE shift of 0.3 eV to the higher BE side of the metallic Au feature.[30] Together with optical properties (including a shift in the surface plasmon resonance), electrical properties, and XPS results, they concluded that the cluster was Au_4Si and was metallic, and that the silicide nanoclusters appeared to be easily converted to a two-phase system (Au and Si) upon annealing above 180 °C.[30] Our XPS data (Figure 3) also indicate that the as-formed Au silicide at the interface is metallic in nature. If the observed Au silicide were nonmetallic, the BE should gradually shift to the higher BE side with decreasing NP size as the result of increasing sputtering time, due to a final-state charging effect. This assertion, however, does not reconcile with our XPS data. If the Au silicide layer remains intact and only Au agglomerates to form NPs during post-annealing, thereby exposing the silicide layer (Figure 4b), the Au 4f peak at a higher BE (corresponding to Au silicide) would be detectable for the as-prepared sample (i.e., before any sputtering). Because no such silicide peak was observed for the NP samples (samples B−D) before sputtering, we conclude that the interfacial Au silicide must undergo agglomeration in concert with the Au top component to form Au NPs upon annealing of the Au film (Figure 4a).

Figure 3E and F shows typical changes in the Au $4f_{7/2}$ peak intensities as functions of sputtering time (depth profiles) for the metallic Au feature at 84.0−84.1 eV and Au silicide feature at 85.1−85.3 eV, respectively. It should be noted that Ar^+ sputtering could be used to reduce the NP size sufficiently (Figure 4c) to expose any underlying quantum-size effect. Except for sample D, the depth profiles of the other three samples all appear to have similar shapes, with considerable reduction for the metallic Au features over the first 60 s of sputtering and plateau-like profiles centering over 60−120 s sputtering for the respective Au−Si features. For sample D, the predominant intensity of the metallic Au top layer undergoes a sharp decrease and becomes almost completely extinct, exposing the Au−Si layer underneath, after just 30 s of sputtering (Figure 3E). Concomitantly, the corresponding Au−Si intensity reaches a maximum after 15 s of sputtering and then reduces to its as-deposited value after 180 s of sputtering (Figure 3F). As expected, the total amount of Au deposition, as reflected by the integrated areas of the metallic Au feature under the depth profiles, is proportional to the sputter-deposition time. The Au $4f_{7/2}$ peak intensity of sample D (obtained with 10 s of sputter-deposition followed by 100 °C post-annealing) is at least 4 times weaker than that of sample A (obtained with 60 s of sputter-deposition). For sample B (also obtained with 60 s of sputter-deposition but followed by 650 °C post-annealing), the metallic Au $4f_{7/2}$ peak is also weaker before sputtering but with considerable intensity reduction over a more extended depth than that for the Au film obtained without the post-annealing (sample A), which is consistent with the lesser areal coverage of the Au NPs, with thicker Au top components, on the substrate. The similar areas found for the two shaded areas clearly indicate that the height and Au layer thickness of the Au NPs (sample B, resulting from post-annealing of the as-deposited film sample A) are larger than those of the corresponding as-deposited Au film (sample A), suggesting agglomeration through droplet formation (Figure 4a). In the case of Au silicide (Figure 3F), the corresponding maximum Au $4f_{7/2}$ peak intensity does not appear to be critically related to the sputter-deposition time. The relative total amounts of Au silicide for individual samples are found to follow those of the corresponding Au deposits, while the extents of Au silicide over depth appear to depend on the annealing temperature (and annealing time). The more limited extent for sample B relative to sample A indicates that the Au NPs in sample B occupy a smaller total footprint (contact area) on the substrate than the uniform film in sample A.

Figure 5 shows the corresponding VB spectra as functions of sputtering time for the four samples. The VB spectra of the four samples after sputtering for over 480 s resemble one another, and are dominated by a prominent feature at 2.7 eV corresponding to Si s-p band, and a strong feature at 9.2 eV corresponding to Ar 3p features of implanted Ar^+ ions. The Ar to Si ratio can be estimated from the Ar 3p and Si 2p XPS intensities and their corresponding sensitivity factors. For example, the relative concentration is found to be 1 Ar atom per 25 Si atoms for the spectra obtained after 960 s sputtering. We believe the extremely low implanted Ar concentration (less than 4%) could not affect the chemical state of the Si species. For the as-deposited Au film (sample A) and Au NP samples (samples B−D), the VB spectra are also found to be similar to one another, with two prominent peaks at 3.6 and 6.2 eV attributed to metallic Au $5d_{5/2}$ and Au $5d_{3/2}$ bands, respectively, in good accord with the characteristic VB features for metallic gold.[25,26] For sample A (Figure 5A), upon sputtering for 30 s, the Au $5d_{5/2}$ band at 3.6 eV shifts to a higher BE while the Au $5d_{3/2}$ peak at 6.2 eV remains essentially unchanged in its BE position. Upon 60 s sputtering, the Au $5d_{5/2}$ band becomes weaker and shifts to 4.2 eV, resulting in a smaller 5d spin−orbit splitting (2.0 eV) than that for metallic Au (2.6 eV). On the basis of the corresponding Au $4f_{7/2}$ peak areas (Figure 3A), the Au silicide to metallic Au population ratio is about 4:6. Continued sputtering of sample A for over 120 s leaves mostly Au silicide on the substrate (Figure 5A), in accord with the Au 4f spectral changes shown in Figure 3A. The corresponding VB spectrum not only becomes weaker but exhibits a markedly different spectral envelope, with the Au $5d_{5/2}$ and $5d_{3/2}$ bands located at 5.3 and 6.6 eV, respectively. With increasing sputtering time, the VB spectrum becomes very weak and evolves to that of the Si substrate after 480 s of sputtering. For the NPs of samples B (Figure 5B) and C (Figure 5C), the respective VB spectral evolutions with sputtering time follow that of sample A, with minor differences in the onsets of the Au silicide and Si substrate features. In case of sample D (Figure 5D), the Au 5d VB peaks change more drastically with sputtering time, with the characteristic VB (and Au 4f) of metallic Au disappearing at a shorter sputtering time, which is due to the smaller Au NPs

(53) Cox, D. M.; Eberhardt, W.; Fayet, P.; Fu, Z.; Kessler, B.; Sherwood, R. D.; Sondericker, D.; Kaldor, A. *Z. Phys. D: At., Mol. Clusters* **1991**, *20*, 385.

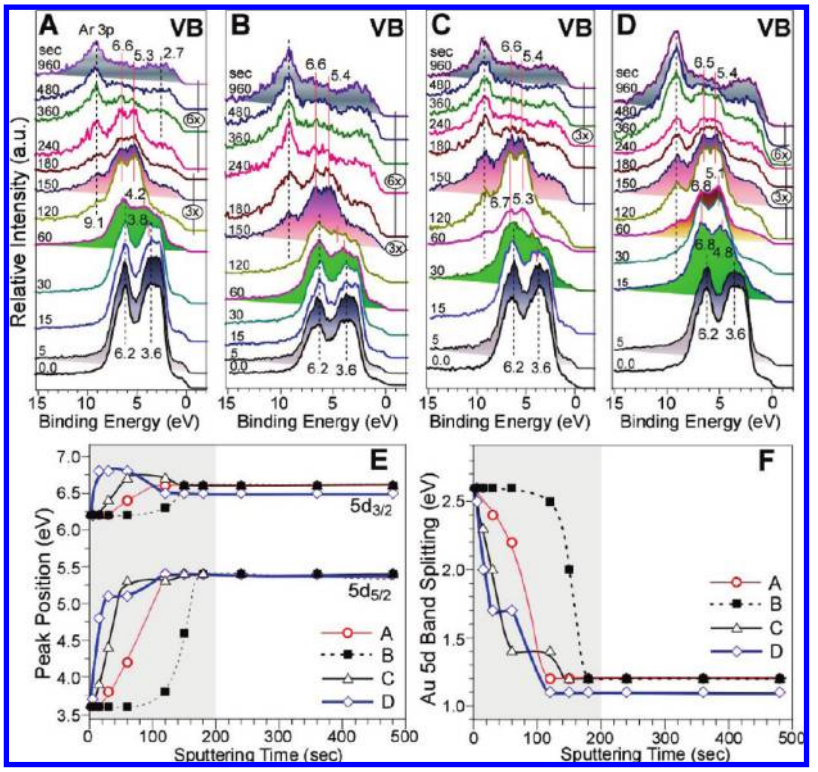

Figure 5. VB spectra collected as a function of Ar^+ sputtering time for (A) a 10 nm thick Au film obtained by sputter-deposition for 60 s, and Au nanoparticle samples obtained with different respective combinations of sputter-deposition time and post-annealing temperatures (for 1 h) of (B) 60 s and 650 °C, (C) 30 s and 550 °C, and (D) 10 s and 100 °C, and (E) their corresponding peak positions of Au $5d_{5/2}$ and $5d_{3/2}$ bands, and (F) their band splitting.

on Si substrate. Upon 15 s of sputtering, the VB bands are located at 4.8 and 6.8 eV with a band splitting of 2.0 eV. These peak positions remain unchanged in the 15−60 s sputtering range with a slight reduction in the relative peak intensity. Upon 120 s sputtering, the two bands with a splitting of ~1.0 eV have become quite similar to the corresponding VB features for other samples shown in Figure 5A−C.

Figure 5E and F shows the BE positions of the Au $5d_{5/2}$ and $5d_{3/2}$ features and their corresponding band splitting, respectively, as functions of sputtering time for the four samples. Evidently, the changes can be divided into two stages, below and above 200 s of sputtering. For sputtering times greater than 200 s, the positions of the Au $5d_{5/2}$ peak at 5.4 eV and Au $5d_{3/2}$ peak at 6.6 eV remain unchanged with sputtering time and are nearly the same for all four samples (Figure 5E). This result is consistent with the presence of Au silicide between the Au component and the Si substrate in all four samples, as indicated by our Au 4f results. In the early stage with sputtering times less than 200 s during which the metallic Au becomes thinner (Figure 4c), the locations of the two Au 5d peaks change more sharply from their metallic Au positions with sputtering time. The BE of the Au $5d_{5/2}$ increases less abruptly (from 6.2 eV) than that of the Au $5d_{3/2}$ (from 3.6 eV) with sputtering time (Figure 5E). Consequently, their corresponding band splitting (spin−orbit splitting) decreases with sputtering time in the early stage (Figure 5F), and the splitting decreases more sharply as the metallic Au becomes thinner, with those of samples D and C being more abruptly changed than samples B and A. Interestingly, for smaller Au NPs, especially sample D (and sample C), the BE of the Au $5d_{5/2}$ band shows a maximum in the sputtering range of 15−60 s, which is 0.3 eV larger than that for Au silicide. For the larger Au NPs and the Au film, the respective BE of Au $5d_{5/2}$ band is not larger than that of Au silicide by more than 0.1 eV. Although the intensity of the Au 4f feature of sample D (Figure 3D) is reduced, their BE positions (and the fwhms) show no discernible change with increasing sputtering time from 60 to 120 s. In contrast, the VB features exhibit a notable change, with the band splitting decreasing from 1.7 eV (6.8−5.1 eV) to 1.1 eV (6.5−5.4 eV) upon increasing sputtering time to 120 s. Obviously, the number density of smaller Au NPs (sample D) is larger than that for larger NPs (e.g., sample B). For the same Au 4f intensity, the average size (or the substrate contact area) of the former is much smaller than the latter. Because the proportion of atoms in each NP in contact with the substrate increases with decreasing particle size, the NPs in sample D are expected to be more directly influenced by the substrate. For this reason, the changes in the VB band splitting could also be due to a substrate effect (e.g., contact area).

Boyen et al. reported two Au 5d valence bands at 4.8 and 6.7 eV for an amorphous $Si_{70}Au_{30}$ alloy.[54] They found that the relative intensities of the two bands depend on the annealing temperature, despite no observable change in their peak positions. This was cautiously attributed to a clustering of Au atoms in amorphous Au−Si alloy. They also found that the Au $5d_{5/2}$ band shifts to a higher BE with decreasing Au content, from 4.4 eV for $Si_{20}Au_{80}$ to 5.2 eV for $Si_{80}Au_{20}$, which is very similar to our present result for the Au $5d_{5/2}$ band shift with increasing sputtering time (Figure 5E). Lee and Hwang calculated the DOS for Au_xSi_{100-x} (with $x = 25, 50, 75$) and attributed the Au 5d shift to a higher BE with decreasing Au content and the stability of the Au−Si alloy to change in the hybridization of Si 3p and Au 5d states.[55] Guczi and co-workers also reported very similar VB spectra to our results for

(54) Boyen, H. G.; Rieger, P.; Haeussler, P.; Baumann, F.; Indlekofer, G.; Oelhafen, P.; Guentherodt, H. J. *J. Phys.: Condens. Matter* **1990**, *2*, 7115.
(55) Lee, S.-H.; Hwang, G. S. *J. Chem. Phys.* **2007**, *127*, 224710.

a 10 nm thick Au film on a native-oxide-covered Si(100) substrate (sample A), along with an increase in the catalytic activity, after Ar^+ ion sputtering.[16,48] They attributed the different VB features from that of metallic Au to the quantum size effect, because ion sputtering reduces the size of Au islands. They further excluded the possibility of Au−Si alloy formation, because the VB feature returned to that of metallic Au after their catalytic tests at high temperature.[16] In addition, they observed that the small Au NPs agglomerate to form larger Au particles, as evidenced by transmission electron microscopy. Because they believed that Au silicide could not convert to metallic Au, they attributed the recovery of metallic Au to the agglomeration of small Au NPs. However, Compagnini et al. showed that Au silicide nanoclusters could easily phase separate to Au and Si upon heating above 180 °C.[30] If the small Au silicide particles could undergo phase separation and agglomeration at high temperature[30] (Figure 4d), the small Au silicide NPs could form larger particles with metallic Au on top and Au silicide at the interface during the catalyst experiment.[48] This alternative phase separation model could also explain the observations of Guczi et al.[16] Although the VB narrowing observed in the present system is clearly due to Au−Si alloy, as supported by our XPS results, it is difficult, in practice, to predict whether the observed spectral changes are due to quantum size or alloying effects, based solely on the evolution in the VB features (e.g., narrowing of Au 5d band splitting). In several studies involving Au/quartz,[20] alkanethiolate-capped Au/carbon,[23] Au/amorphous carbon,[38] Au/carbon nanotubes,[39] and Au/diamond,[56] the researchers claimed that the narrowing of the Au 5d band is due to the quantum size effect and not to the formation of alloys (such as Au silicide).

The formation of Au alloy has also been observed on other substrates. By depositing a Au film with different coverage on a Ge substrate, Ruckman et al. found that the Au 5d band splitting gradually increases from 1.5 to 2.2 eV as the Au coverage increases from 0.5 to ∼20 Å.[57] Their VB features for the low Au coverage are found to be very similar to our VB spectra for Au NPs in sample D (Figure 5D). For their corresponding Au 4f spectra at low Au coverage, they observed a 4f component at 0.9 eV higher BE than that of bulk gold, which is also in good accord with that (1.0 eV) observed for Au silicide (Figure 3D). They attributed these Au 4f and VB features to a Au−Ge mixture species, such as Au_3Ge.

Figure 6 shows the DOS near the Fermi level for the Au NP sample with the smallest size range of 6−12 nm (sample D). As expected, the DOS decreases near the Fermi edge as the metallic Au component is reduced by Ar^+ sputtering during the depth-profiling experiment. According to the Au 4f spectra (Figure 3D), sputtering for 30 s would remove the entire metallic Au component. However, considerable DOS at the Fermi level is observed after 30 s of sputtering, indicating that the Au silicide that remains is not an insulator. Although the DOS decreases further with increasing sputtering time, no evidence of any metal-to-nonmetal transition with increasing sputtering time (or decreasing size) can be found. If such a transition were to occur, the Au 4f of Au silicide should also shift to a higher BE due to a final-state charging effect. Such a shift has not been observed in the present work, and the Au 4f peak position remains unchanged with sputtering time (Figure 3). The present observation is in contrast to the study by Zhang and Sham, who reported a metal-to-insulator transition in the DOS at the Fermi level for alkanethiolate-capped Au NPs of 1.6 nm in size.[23] The effect of the substrate, particularly in facilitating the formation of Au silicide, therefore plays a crucial role in the observed electronic structure near the Fermi edge.

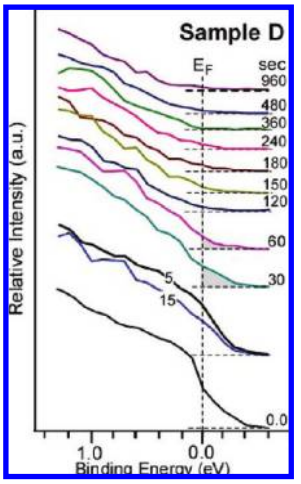

Figure 6. DOS near the Fermi level for the Au NP sample obtained by 10 s of sputter-deposition followed by 100 °C annealing.

4. Summary

Gold NPs over an extended average size regime from 8 to 48 nm have been prepared on a native-oxide-covered Si(100) substrate by using a simple method, involving magnetron sputter-deposition followed by thermal annealing. SEM shows near-regularly spaced NPs with a fairly uniform size distribution and interparticle separations linearly dependent on the average size, while GIXRD confirms the nanocrystalline nature of the fcc metallic Au grains. Detailed depth-profiling XPS studies show that the new Au 4f peak located at 85.0 eV, 1.1−1.2 eV higher in BE than that of metallic Au, can be attributed to the formation of Au silicide at the interface between Au and Si. The Au 4f depth profiles further reveal that the transition from metallic Au to Au silicide occurs over a short sputtering time range, indicating that the silicide interface is abrupt. No clear evidence for the quantum size effect was observed. The corresponding Au $5d_{5/2}$ VB is found to shift to a higher BE (5.4 eV) with the Au $5d_{3/2}$ band located at 6.6 eV, causing a narrower 5d band splitting (1.2 eV). Although narrowing of the Au 5d band splitting has also been attributed to the quantum size effect in earlier studies on Si and other substrates, the reduction in the band splitting in the present system can best be explained by the emergence of Au silicide at the interface. From the finite DOS at the Fermi level and the constant Au $4f_{7/2}$ peak position, we conclude that Au silicide is metallic-like. These near-regularly spaced Au NPs on a substrate could serve as a simple conductive and chemically reactive template for potential applications in nanoelectronics and catalysts.

Acknowledgment. This work was supported by the Natural Sciences and Engineering Research Council of Canada.

(56) Boyen, H.-G.; Herzog, Th.; Kastle, G.; Weigl, F.; Ziemann, P.; Spatz, J. P.; Moller, M.; Wahrenberg, R.; Garnier, M. G.; Oelhafen, P. *Phys. Rev. B* **2002**, *65*, 075412.

(57) Ruckman, M. W.; Joyce, J. J.; Boscherini, F.; Weaver, J. H. *Phys. Rev. B* **1986**, *34*, 5118.